

# Getting Closer to the Real Bacterial Cell Wall Target: Biomolecular Interactions of Water-Soluble Lipid II with Glycopeptide Antibiotics

Pauline J. Vollmerhaus,<sup>[a]</sup> Eefjan Breukink,<sup>[b]</sup> and Albert J. R. Heck\*<sup>[a]</sup>

**Abstract:** A novel synthesized water-soluble variant of lipid II (LII) was used to evaluate the noncovalent interactions between a number of glycopeptide antibiotics and their receptor by bioaffinity electrospray ionization mass spectrometry (ESI-MS). The water-soluble variant of lipid II is an improved design, compared to the traditionally used tripeptide *N,N'*-diacetyl-L-lysyl-D-alanyl-D-alanine (KAA), of the target molecule on the bacterial cell wall. A representative group of glycopeptide antibiotics was

selected for this study to evaluate the validity of the novel cell-wall-mimicking target LII. Structure–function relationships of various glycopeptide antibiotics were investigated by means of 1) bioaffinity mass spectrometry to evaluate solution-phase molecular interactions with both LII and KAA, 2) fluorescence

leakage experiments to study the interactions with the membrane-embedded lipid II, and 3) minimum inhibitory concentrations against the indicator strain *Micrococcus flavus*. Our results with the novel LII molecule reveal that some antibiotics interact differently with KAA and LII. Additionally, our data cast doubt on the hypothesis that antibiotic self-dimerization assists in the in-vivo efficacy. Finally, the water-soluble lipid II proved to be a better model of the bacterial cell wall.

**Keywords:** antibiotics • dimerization • glycopeptides • lipid II • molecular recognition

## Introduction

Glycopeptide antibiotics (Figure 1) are structurally characterized by a macrocyclic peptide backbone with sugar moieties attached at various sites.<sup>[1]</sup> With the exception of amino acid residues 1 and 3, and the number of linked sugars, there is a high degree of homology within this class of molecules. The clinical application of vancomycin, the prototypical glycopeptide antibiotic, is in the treatment of methicillin-resistant *Staphylococcus aureus* (MRSA).

Glycopeptide antibiotics target the bacterial cell wall of Gram-positive bacteria, which is a three-dimensional network consisting of building blocks of *N*-acetylglucosamine (GlcNAc) and *N*-acetylmuramic acid (MurNAc) that are assembled in the cytosol. When the nucleotide-activated molecules UDP-GlcNAc and UDP-MurNAc-pentapeptide are joined via the C<sub>55</sub>-lipid carrier undecaprenyl phosphate,

they form lipid II (Figure 2), which is then transferred from the cytoplasm to the outer surface of the membrane<sup>[2]</sup> where it becomes available to the cell-wall synthesis machinery. The specific target of vancomycin, and related antibiotics, is the pentapeptide terminating in L-Lys-D-Ala-D-Ala attached to the MurNAc amino sugar. It is believed that the antibiotic activity of the drugs is primarily a result of these (multivalent) noncovalent interactions with L-Lys-D-Ala-D-Ala.<sup>[3]</sup> Bacterial resistance to vancomycin occurs when the terminal residue has mutated to D-Ala-D-lactate, as in the case of vancomycin-resistant *enterococci* (VRE).<sup>[4]</sup>

Besides the strong affinity of glycopeptide antibiotics for the L-Lys-D-Ala-D-Ala terminus on LII, it has been proposed that the tendency of these antibiotics to form dimers promotes their ability to eradicate bacteria.<sup>[5–7]</sup> Additionally, it has been shown that the presence of bacterial cell wall analogues generally enhances the dimerization of glycopeptide antibiotics.<sup>[8–10]</sup>

Apart from target recognition and dimerization, the chemical nature of the linked carbohydrates is thought to have a possible influence on the antibacterial efficacy of the antibiotics. It has been suggested that the sugars attached to the antibiotics may provide selectivity in binding cell-wall precursors terminating in D-Ala-D-Ala and are probably involved in stabilizing the dimer.<sup>[6]</sup>

Glycopeptide antibiotics are not the only antimicrobials to use lipid II to weaken the structural integrity of the bacterial wall. Recently, it has been shown that nisin, a lanthionine-

[a] Prof. Dr. A. J. R. Heck, P. J. Vollmerhaus  
Department of Biomolecular Mass Spectrometry  
Bijvoet Center for Biomolecular Research and  
Utrecht Institute for Pharmaceutical Sciences, Utrecht University  
Sorbonnelaan 16, 3584 CA Utrecht (The Netherlands)  
Fax: (+31)30-251-8219  
E-mail: a.j.r.heck@chem.uu.nl

[b] E. Breukink  
Center of Biomembranes and Lipid Enzymology  
Department of Biochemistry of Membranes  
Institute for Biomembranes, University of Utrecht  
Padualaan 8, 3584 CH Utrecht (The Netherlands)

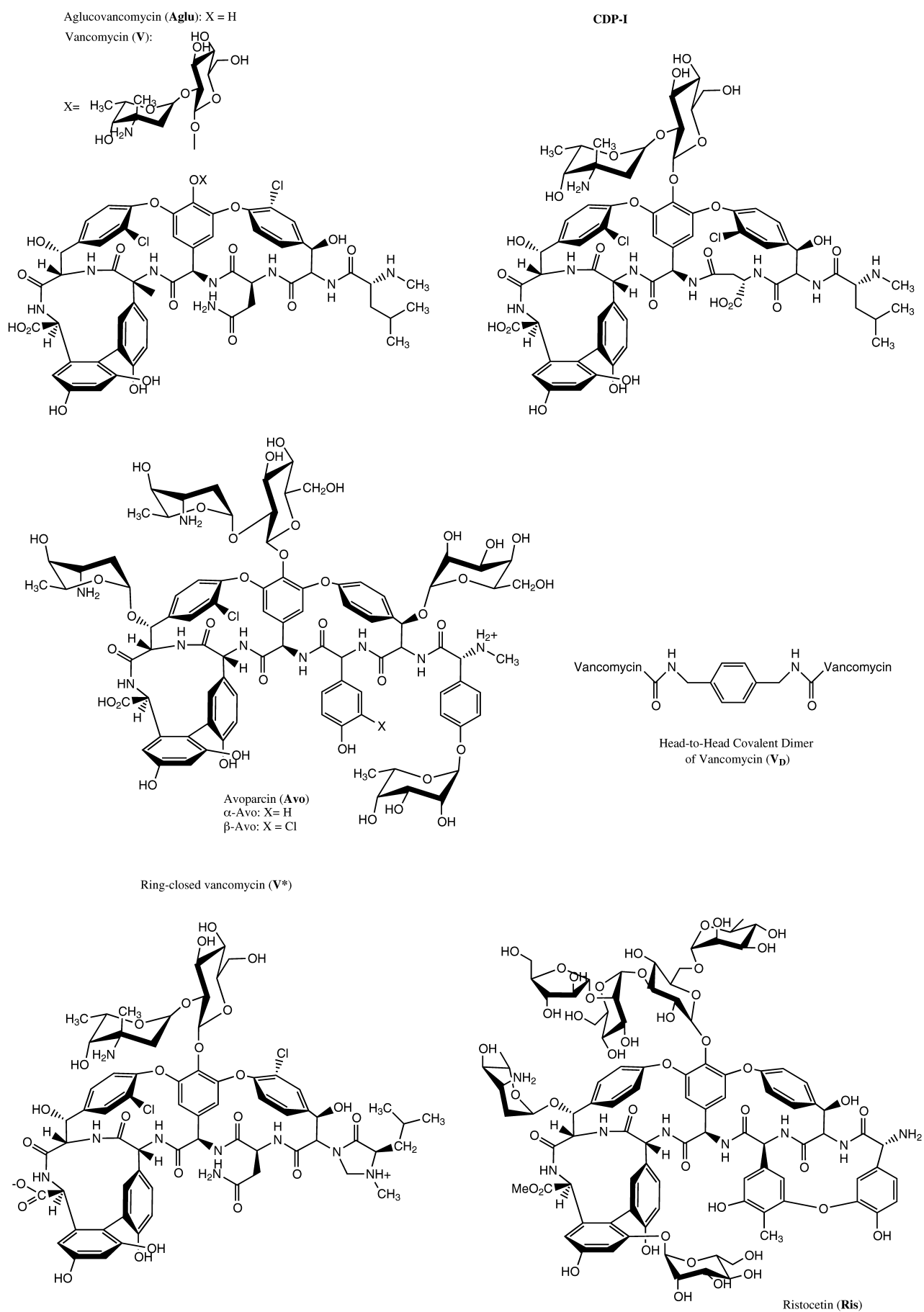


Figure 1. Chemical structures of the glycopeptide antibiotics used in this study.

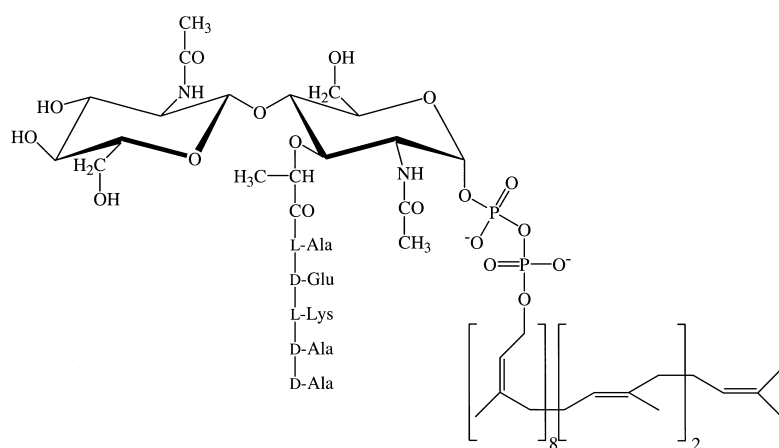


Figure 2. Chemical structure of lipid II. The newly synthesized water-soluble form of lipid II contains only three isoprene units in the tail as opposed to the eleven in the natural form.

containing antibiotic, interacts with lipid II to form pores in the bacterial membrane leading to cell death.<sup>[11, 12]</sup> While having completely different mechanisms of action, glycopeptide antibiotics inhibit the pore-forming ability of nisin. This competitive inhibition is presumably caused by the fact that they both interact with lipid II, albeit at different binding sites. Bacterial cell-wall-mimicking peptides, such as *N,N'*-diacetyl-L-lysyl-D-alanyl-D-alanine (KAA), can be used to study the affinity of glycopeptides and the structural changes upon binding of the glycopeptides in vitro by a variety of analytical techniques, including NMR, calorimetry, and mass spectrometry.<sup>[9, 13–21]</sup> In this work we compare the interactions of a set of glycopeptide antibiotics towards the traditionally used model target, the bacterial cell-wall-mimicking peptide KAA and a novel model target, a water-soluble variant of lipid II. The water-soluble form contains a prenyl chain which is three units long as opposed to the eleven units in the wild-type form of lipid II. This is the first report of glycopeptide antibiotic interactions with water-soluble lipid II. A representative group of glycopeptide antibiotics, that touch each facet of the efficacy-determining parameters described above, have been selected for this study. Our investigation uses mass spectrometry to evaluate solution-phase molecular interactions, fluorescence (leakage) to study the interactions with membrane-embedded wild-type lipid II and minimum inhibitory concentrations to determine antibiotic efficacy against the indicator strain *Micrococcus flavus*. By comparing the data obtained by these orthogonal methods, we seek insight into the structure–function relationships of glycopeptide antibiotics.

## Results

A representative set of seven glycopeptide antibiotics (Figure 1) was selected to investigate the structural features that influence the antibiotic molecular interaction with both the model and our novel, bacterial cell-wall-mimicking targets. Each antibiotic embodies one or more aspects of the efficacy-determining molecular parameters exhibited by this class of antibiotics, including target specificity, presence of sugar

residues, and dimerization properties. A range of target ligand affinity and antimicrobial activity is demonstrated by the selected glycopeptides, as will be described below. Vancomycin (**V**) was selected as the prototypical glycopeptide antibiotic. Avoparcin (**Avo**)<sup>[4, 22, 23]</sup> and ristocetin (**Ris**)<sup>[24]</sup> were selected because they contain a higher number of carbohydrate moieties. In contrast to **Avo** and **Ris**, aglucovancomycin (**Aglu**) was chosen because it lacks the presence of any carbohydrate moieties. The synthesized head-to-head covalent dimer of van-

comycin (**V<sub>D</sub>**) is included to assess the effect of dimerization on biological activity.<sup>[8]</sup> Two glycopeptides with damaged or inactive binding pockets were chosen for comparison with active glycopeptides: a formaldehyde-modified derivative of vancomycin (**V\***) containing a ring-closed imidazolidinone at the N-terminus,<sup>[25]</sup> and **CDP-I**, a biologically inactive degradation product of vancomycin<sup>[26]</sup> resulting from an unusual aspartic-to-isoaspartic rearrangement at the third residue.

**Antimicrobial efficacy:** As an initial assessment of the antibiotic efficacy of our set of glycopeptide antibiotics, minimum inhibitory concentrations (MICs) were determined against the indicator strain *Micrococcus flavus*. The results from the MIC experiments are shown in Table 1. **V<sub>D</sub>**, **V**, and

Table 1. Minimum inhibitory concentrations (MIC) of the glycopeptide antibiotics used against *Micrococcus flavus*.

Antibiotic	MIC [ $\mu\text{g mL}^{-1}$ ]
<b>V<sub>D</sub></b>	0.42 ± 0.04
<b>Ris</b>	0.16 ± 0.12
<b>Avo</b>	0.33 ± 0.11
<b>V</b>	0.39 ± 0.08
<b>V*</b>	1.44 ± 0.4
<b>Aglu</b>	1.6 ± 0.06
<b>CDP-I</b>	> 3

**Avo** behaved similarly with MIC values of 0.42 ± 0.04, 0.39 ± 0.08, and 0.33 ± 0.11  $\mu\text{g mL}^{-1}$ , respectively. Against *M. flavus*, **Ris** was three times more active than **V** with a MIC value of 0.16 ± 0.12  $\mu\text{g mL}^{-1}$ . In contrast, the concentrations required to inhibit bacterial growth for **V\*** and **Aglu** were on the order of five times higher, indicating that some antibacterial activity is retained. **CDP-I** was the least active of our set of antibiotics.

**Molecular interactions probed by mass spectrometry:** Electrospray is a gentle ionization technique that allows even relatively weak noncovalent complexes to remain intact as they are transferred into the gas phase, prior to analysis by mass spectrometry. Several groups, including ours, have used bioaffinity ESI-MS methodology previously to evaluate the

strength of the interactions between some glycopeptide antibiotics and D-Ala-D-Ala-terminated peptides.<sup>[13–16, 25, 27]</sup> Rather than using the D-Ala-D-Ala peptide models for the bacterial cell wall, one would like to study the interactions of glycopeptide antibiotics with intact lipid II. Unfortunately, intact lipid II is insoluble in water and therefore not amenable to analysis by bioaffinity electrospray mass spectrometry. The recently reported synthesis of a water-soluble variant of lipid II<sup>[28]</sup> allows, for the first time, a more comprehensive characterization of the molecular interactions that underlie glycopeptide antibiotic efficacy.

A primary assumption for the determination of association constants by mass spectrometry is that the ionization probability of the free antibiotic is equivalent to that of the antibiotic–ligand complexes. This assumption has been validated for the vancomycin/D-Ala-D-Ala system by performing different quantitative measurements at different concentrations of antibiotics and ligands.<sup>[29]</sup> A limitation to determining association constants by mass spectrometry includes the fact that the ion response decreases with increasing  $m/z$  values. Several factors contribute to this effect, including ionization efficiency, mass transfer efficiency, detector response, instrument type, and tuning parameters. Therefore, it is likely that there will be some mass discrimination against higher  $m/z$  values. Careful control of all experimental parameters is necessary to maintain a balance between ion desolvation and complex dissociation with respect to the ion source parameters thus permitting quantification. In many cases, relative ion intensities of the different complexes

observed in the mass spectra correlate well with the equilibrium distribution of complexes in solution. It has also been observed that proteins or peptides of comparable size and amino acid content have similar electrospray ionization response factors.<sup>[30]</sup> For compounds that bind to target molecules with similar-type binding mechanisms, it is likely that they have similar gas-phase stabilities, and consequently allow a relative assessment of the binding affinities of the antibiotics towards the bacterial cell-wall-mimicking ligands.<sup>[31]</sup> Given the aforementioned considerations, we employed mass spectrometry to investigate the noncovalent complexes formed between the glycopeptide antibiotics and LII, and compared them with those formed with the traditional KAA model peptides.

**Association constants ( $K_A$ ) determined for glycopeptide antibiotics:** The relative  $K_A$  values of **Ris** and **V** were measured by keeping the concentrations of the two glycopeptides constant and titrating in KAA and LII. Previous NMR and MS studies on **Ris** and **V** demonstrated that heterodimers might be formed both in the presence and absence of the peptide ligand.<sup>[14, 32]</sup> In our spectra, any heterodimer ( $m/z$  1172, triply protonated) formation observed was less than 10% of the total signal and was therefore excluded from our calculations. Figure 3A shows the mass spectrum of equimolar concentrations of **V** ( $m/z$  725, doubly protonated) and **Ris** ( $m/z$  1034, doubly protonated) without any ligand present. Figure 3B shows that the addition of KAA induces the development of the **V**-KAA complex ( $m/z$  910,

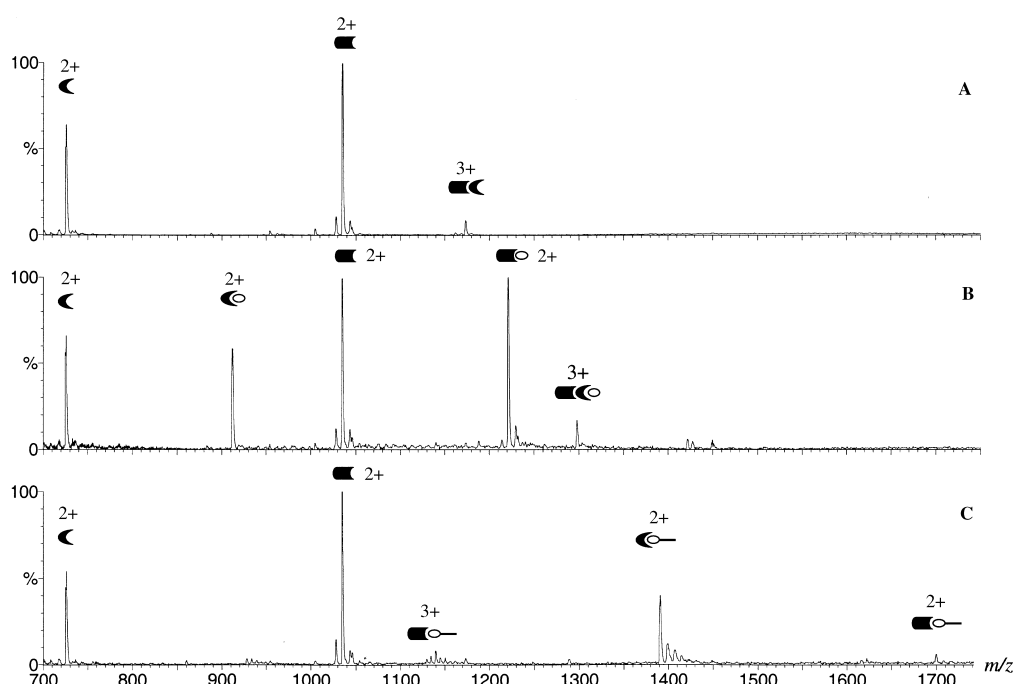


Figure 3. ESI mass spectra of **A**. Mixture of 10  $\mu\text{M}$  **V** (●, free **V**) and **Ris** (■, free **Ris**). The doubly protonated **V** and **Ris** can be observed at  $m/z$  725 and  $m/z$  1034, respectively. The triply protonated heterodimer formed between **V** and **Ris** (○, **Ris-V** heterodimer) can be found at  $m/z$  1172. **B**. Competition experiment between **V** and **Ris** after adding 16  $\mu\text{M}$  KAA (○, free KAA). The doubly protonated complex of **V** with KAA (■●, **V-KAA** complex) and **Ris** with KAA (●●, **Ris-KAA** complex) can be found at  $m/z$  910 and  $m/z$  1220, respectively. A triply protonated species belonging to the complex of the heterodimer with KAA can also be seen at  $m/z$  1297 (●●○, **Ris-V-KAA** complex). **C**. Competition experiment between **V** and **Ris** after adding 8  $\mu\text{M}$  LII (■●○, free LII). The doubly protonated complex of **V** with LII (●●○, **V-LII** complex) and **Ris** with LII (■●○, **Ris-LII** complex) can be found at  $m/z$  1390 and  $m/z$  1700, respectively. The triply protonated species of the complex of **Ris** with LII is also observed ( $m/z$  1139).

doubly protonated) and the **Ris**-KAA ( $m/z$  1220, doubly protonated) complex. The ratio of free to complexed glycopeptide is 1.3:1 and 0.94:1 for **V** and **Ris**, respectively. However, when LII is added (Figure 3C), the complex between **V** and LII ( $m/z$  1390, doubly protonated) is preferred over that of **Ris** and LII ( $m/z$  1700, doubly protonated,  $m/z$  1134, triply protonated). The ratio of free to complexed glycopeptide for **V** is now 0.77:1, whereas it is almost 20:1 for **Ris**. This is remarkable because it is well documented that **V** and **Ris** behave similarly towards KAA bacterial cell-wall mimics.<sup>[18, 32–36]</sup> From the titration experiments, the  $K_A$  values determined for **Ris** and **V** complexed with KAA were  $0.43 \pm 0.09 \mu\text{M}^{-1}$  and  $0.40 \pm 0.08 \mu\text{M}^{-1}$  respectively. In contrast, **V** has a higher  $K_A$  for LII at  $1.1 \pm 0.2 \mu\text{M}^{-1}$ . The  $K_A$  determined for **Ris** with LII was  $0.24 \pm 0.05 \mu\text{M}^{-1}$ .

Similarly, we attempted to determine the  $K_A$  of  $\mathbf{V}_D$  for KAA, by holding the dimer concentration constant at  $10 \mu\text{M}$  and titrating in the two different ligands. The observed behavior of  $\mathbf{V}_D$  towards the two ligands was significantly different. The mass spectra from a titration experiment with KAA are depicted in Figure 4. In the top mass spectrum, the only observed ion signals are those of the  $3^+$  peak of  $\mathbf{V}_D$  ( $m/z$  1000) and its ammoniated counterpart ( $m/z$  1005), and the  $2^+$  peak of  $\mathbf{V}_D$  ( $m/z$  1500). As KAA is added, the gradual formation of complexes can be observed. At  $8 \mu\text{M}$  KAA, the majority of the complexes formed consist of a singly bound KAA to a covalent dimer (1:1,  $m/z$  1124, triply protonated) with a smaller amount of fully occupied  $\mathbf{V}_D$  (1:2,  $m/z$  1248, triply protonated) binding. At  $16 \mu\text{M}$  KAA, the dominant species is a 1:2 complex, signifying that both binding sites are occupied. Notably, as the concentration of KAA increases,  $\mathbf{V}_D$

begins to dimerize, as is evident from the formation of the observed species  $[\mathbf{V}_D(\text{KAA})_2]_2$  ( $m/z$  1497, quintuply protonated). The evolution of the different  $\mathbf{V}_D$ -KAA complexes as a function of the KAA concentration is shown in Figure 5. Dimerization appears to be preceded by the total occupation of the monomeric  $\mathbf{V}_D$  binding sites.

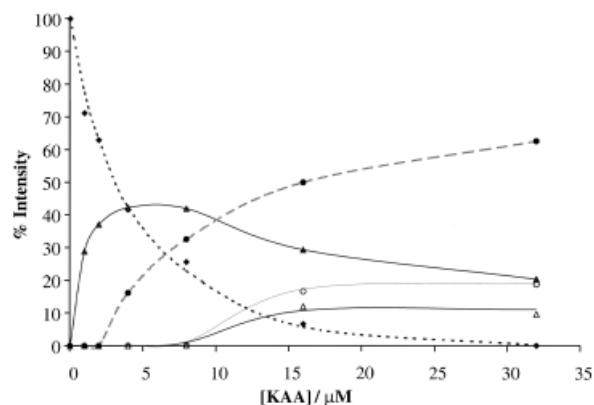


Figure 5. Intensities of different KAA species observed in the ESI mass spectra as a function of increasing KAA concentration;  $\mathbf{V}_D$  ( $\blacklozenge$ ),  $\mathbf{V}_D\text{KAA}$  ( $\blacktriangle$ ),  $\mathbf{V}_D(\text{KAA})_2$  ( $\bullet$ ),  $(\mathbf{V}_D)_2(\text{KAA})_3$  ( $\triangle$ ),  $(\mathbf{V}_D\text{KAA})_2$  ( $\circ$ ).

For comparison,  $\mathbf{V}_D$  was titrated with LII. In the bottom mass spectrum of Figure 6 both the  $\mathbf{V}_D(\text{LII})$  complex (1:1,  $m/z$  1443, triply protonated) and the  $\mathbf{V}_D(\text{LII})_2$  complex (1:2,  $m/z$  1887, doubly protonated and 1415, triply protonated) are observed. In contrast to KAA, LII does not appear to induce dimerization of  $\mathbf{V}_D$ , even at excess concentration of lipid II.

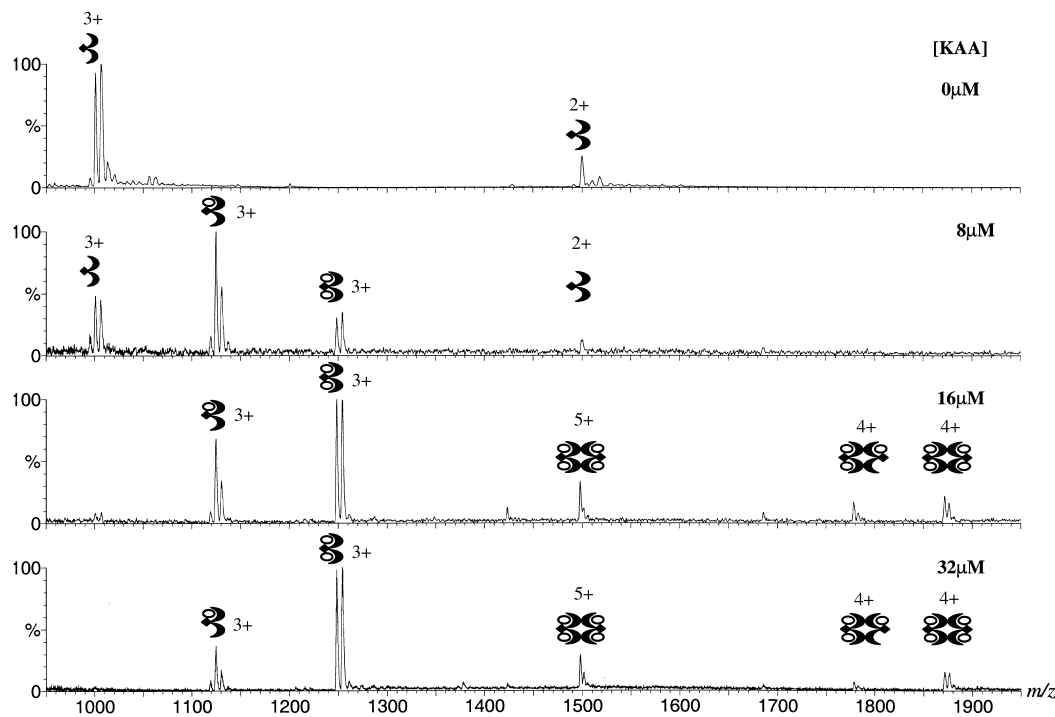


Figure 4. ESI-MS of  $10 \mu\text{M}$   $\mathbf{V}_D$  ( $\text{V}_D$ ), free  $\mathbf{V}_D$  ( $\text{V}_D$ ) titrated with KAA. Initially, the doubly and triply charged peaks for the free  $\mathbf{V}_D$  can be seen at  $m/z$  1000 and  $m/z$  1500. Ammonia adducts are of equal intensity in some cases. With increasing concentration of KAA, triply protonated species of the complex containing a single bound tripeptide ( $m/z$  1124,  $\text{V}_D\text{KAA}$ ), free KAA ( $\text{KAA}$ ) or two bound tripeptides ( $m/z$  1248,  $\text{V}_D(\text{KAA})_2$ ) develop. As the titration is taken further,  $\mathbf{V}_D$  dimerizes and complexes containing three tripeptides ( $m/z$  1778,  $(\text{V}_D)_2(\text{KAA})_3$ ) and even four KAA molecules ( $m/z$  1497,  $(\text{V}_D\text{KAA})_2$ ) are observed.

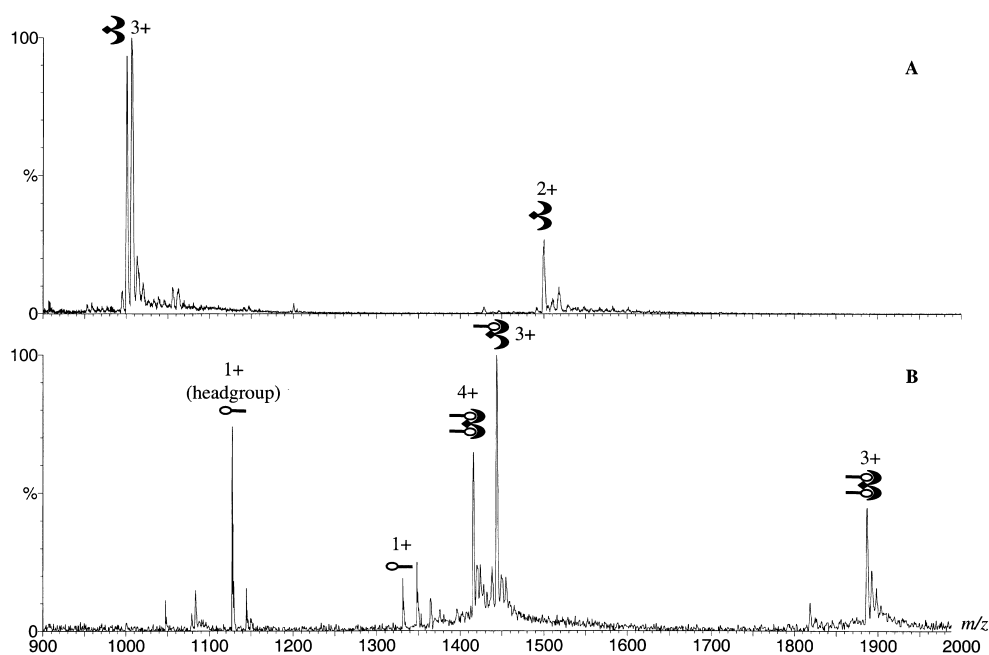


Figure 6. ESI-MS of **A**.  $10\ \mu\text{M}$   $\text{V}_D$  ( $\text{V}_D$ , free  $\text{V}_D$ ). The triply protonated species can be observed at  $m/z$  1000. An ammonia adduct of the triply protonated dimer can be found at approximately  $m/z$  1006 **B**.  $10\ \mu\text{M}$   $\text{V}_D$  combined with  $16\ \mu\text{M}$  LII. The triply protonated complex of  $\text{V}_D$  with one LII molecule attached ( $\text{V}_D$ , free LII) can be found at  $m/z$  1443. The triply and quadruply protonated complex of  $\text{V}_D$  with two LII molecules ( $\text{V}_D$ ) attached can be found at  $m/z$  1887 and  $m/z$  1443, respectively. The singly protonated lipid II ( $\text{LII}$ ) ligand and that of its head group are found at  $m/z$  1331 and  $m/z$  1127, respectively.

The  $K_A$ 's determined for  $\text{V}_D$  with KAA and LII were, however, comparable and found to be  $1.30 \pm 0.26\ \mu\text{M}^{-1}$  and  $1.27 \pm 0.25\ \mu\text{M}^{-1}$ , respectively.

In the competition experiments involving **Avo** and **V**, **Avo** is a mixture of  $\alpha$ - and  $\beta$ -avoparcin where  $\beta$  differs from  $\alpha$  by the substitution of a Cl for an H on one of the rings. Both  $\alpha$ - and  $\beta$ -avoparcin behave as expected towards KAA, where  $\beta$ - is approximately three times more active than  $\alpha$ -avoparcin. In the presence of LII, the association constant of  $\alpha$ -avoparcin is slightly higher, as shown in Table 2. The association constants of our entire set of glycopeptide antibiotics were determined and are summarized in Table 2. For **CDP-I** and **V\***, only very weak complexation with the ligands was observed. The affinity constant for **Aglu** towards KAA was three times less than that of **V**, in agreement with data cited previously in the literature.<sup>[6, 37]</sup> **Aglu** was found to have a higher affinity for LII than for KAA, nevertheless, it is still nearly 10 times lower than that of **V**.

Table 2. Solution-phase binding constants of glycopeptide antibiotics determined by ESI-MS.

Antibiotic	$K_{\text{KAA}} [\mu\text{M}^{-1}]$	$K_{\text{LII}} [\mu\text{M}^{-1}]$
<b>V<sub>D</sub></b>	$1.30 \pm 0.26$	$1.27 \pm 0.25$
<b>Ris</b>	$0.43 \pm 0.09$	$0.24 \pm 0.05$
$\alpha$ - <b>Avo</b>	$0.17 \pm 0.04$	$0.26 \pm 0.05$
$\beta$ - <b>Avo</b>	$0.46 \pm 0.09$	$0.41 \pm 0.08$
<b>V</b>	$0.40 \pm 0.08$	$1.10 \pm 0.2$
<b>V*</b>	$< 0.001$	$< 0.001$
<b>Aglu</b>	$0.01 \pm 0.01$	$0.14 \pm 0.03$
<b>CDP-I</b>	$< 0.001$	$< 0.001$

### Inhibitive effect of glycopeptide antibiotics on nisin-induced membrane leakage:

The antimicrobial agent nisin induces pore formation in bacteria. This pore formation is highly effective if LII is available to nisin.<sup>[11]</sup> It was shown that **V** has an inhibitive effect on nisin's pore-forming ability, presumably because the two antibiotics bind to lipid II, although most likely to different sites. Here, we used this inhibitive effect of **V** on nisin as a measure of the affinity of **V** for LII in a membrane context. The extent of the antagonistic effect of the different glycopeptide antibiotics on nisin's efficacy was determined by measuring the amount of leakage from carboxyfluorescein-filled vesicles as a function of the glycopeptide concentration (Figure 7). From these plots,  $K_{\text{inhibition}}$  values were determined and are given in Table 3.

$K_{\text{inhibition}}$  values were defined as the concentration of glycopeptide antibiotic required to obtain 50% inhibition of the nisin activity. (For clarity, the **Ris** and **Avo** curves were excluded from Figure 7).

Table 3. Inhibition constants for nisin's pore-forming ability determined from carboxyfluorescein leakage experiments.  $K_{\text{inhibition}}$  refers to the concentration of glycopeptide antibiotic required to inhibit nisin activity by 50%.

Antibiotic	$K_{\text{inhibition}} [\mu\text{M}]$
<b>V<sub>D</sub></b> <sup>[a]</sup>	$0.09 \pm 0.02, 0.10 \pm 0.02$
<b>Ris</b>	$0.36 \pm 0.3$
<b>Avo</b>	$0.34 \pm 0.1$
<b>V</b>	$0.46 \pm 0.09$
<b>V*</b>	$15.0 \pm 6.4$
<b>Aglu</b>	$1.35 \pm 0.6$
<b>CDP-I</b>	$\infty$

Both **Avo** ( $0.34 \pm 0.1\ \mu\text{M}$ ) and **Ris** ( $0.36 \pm 0.3\ \mu\text{M}$ ) had a slightly greater inhibitive effect on nisin than **V** ( $0.46 \pm 0.09\ \mu\text{M}$ ). Three times as much **Aglu** ( $1.35 \pm 0.6\ \mu\text{M}$ ) than **V** was required to inhibit nisin to the same extent. Of the glycopeptides studied, **V<sub>D</sub>** had the largest inhibitive effect on nisin pore formation. **CDP-I** had no effect on nisin activity, whereas **V\*** inhibited nisin to a maximum of 40%.

## Discussion

In this work, we examined the molecular interactions and efficacy of a representative set of glycopeptide antibiotics

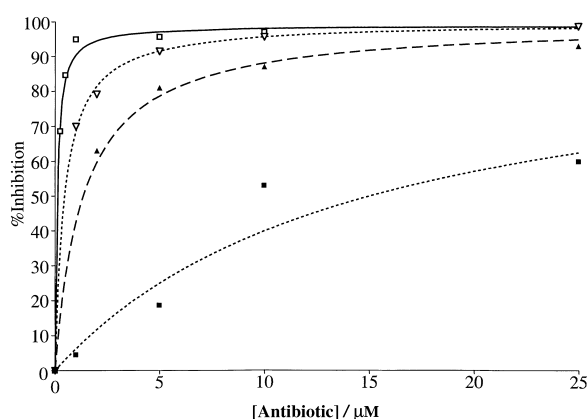


Figure 7. Inhibition of nisin's pore-forming activity by glycopeptide antibiotics as a function of the glycopeptide antibiotic concentration; **V<sub>D</sub>** (□), **Aglu** (▲), **V** (▽), **V\*** (■).

with the bacterial cell wall manifested in different forms (e.g. in vitro MICs, target-mimicking peptides, and model membranes that have incorporated wild-type lipid II). The combination of data reveals some striking new features surrounding the relationship of these glycopeptide antibiotics with bacterial cell-wall models. To date, the model peptide *N,N'*-diacetyl-L-Lys-D-Ala-D-Ala has been used often to evaluate solution-phase interactions between glycopeptide antibiotics and the bacterial cell wall. In this paper, we have used a novel cell-wall-mimicking peptide, a water-soluble variant of lipid II, whose structure differs from the wild type simply by a shorter hydrocarbon tail. There are some inconsistencies in the interactions of the glycopeptide antibiotics with LII as compared to KAA.

The primary interaction of glycopeptide antibiotics is with the D-Ala-D-Ala terminus of lipid II.<sup>[1]</sup> A number of secondary features have been suggested to enhance the potency of glycopeptide antibiotics. For example, the sugar residues may positively influence glycopeptide binding to the bacterial cell wall, as well as possibly interfering with the *trans*-glycosylation process during the formation of the peptidoglycan.<sup>[6, 38]</sup> Another factor that contributes to antibiotic efficacy is the possibility of noncovalent dimerization of some glycopeptide antibiotics.<sup>[39]</sup> It has been reported in the literature that cooperativity may induce glycopeptide antibiotics to dimerize upon binding to bacterial cell-wall analogues.<sup>[40]</sup> There appears to be a subtle balance among these different mechanisms that determines the actual antibacterial activity of each individual glycopeptide.

Previous studies have shown that the binding of KAA to vancomycin involves several intermolecular hydrogen bonds originating from the backbone amides of the antibiotic to the carboxylate anion and amides of the KAA ligand. Structural changes within the binding pocket of vancomycin can result in a dramatic decrease in the ligand binding affinity. In this investigation, **CDP-I** and **V\*** were included because of their diminished target recognition abilities. Indeed, our mass spectrometry experiments confirm that both **CDP-I** and **V\*** bind extremely weakly to KAA and LII. Surprisingly, **V\*** still had an inhibitive effect on nisin pore formation and some vestiges of antibiotic activity. It is likely that the disparity

between **V\*** and **CDP-I** may originate from conformational differences within the binding pocket. **V**, being the prototypical glycopeptide antibiotic, has the optimal configuration for binding KAA. In **CDP-I**, the conformation of the binding pocket has been altered in such a way that the intermolecular distances for hydrogen bond formation between antibiotic and ligand is clearly less optimal. One can only surmise that in the case of **V\***, more of the binding region may be preserved than that of **CDP-I**, allowing **V\*** to interact more, although also weakly, with the bacterial cell-wall target in the different forms presented here. Additionally, it may be possible that the ring closure occurring in **V\*** may be reversible to some extent.

The binding sites of **V** and **Ris** have been shown to be very similar despite differences in structure.<sup>[33]</sup> The binding pocket created in **V** when attaching KAA ligand contains hydrophobic interaction sites formed from aromatic and aliphatic hydrocarbon groups thus strengthening the hydrogen bonds. In the case of **Ris**, the walls of the pocket are formed from aromatic hydrocarbon groups.<sup>[33]</sup>

In our experiments, **V** and **Ris** exhibit differences in affinity with respect to complex formation with LII and KAA. For binding to KAA, **V** and **Ris** have nearly identical association constants. However, **V** clearly has a higher affinity than **Ris** for LII. If we propose LII to be a more descriptive mimic of the bacterial cell wall, then plainly **V**'s target-recognition ability is stronger than that of **Ris**. Despite of this, **Ris** is a more effective antibiotic against *Micrococcus flavus*, as demonstrated by the MICs. This concept of dominant behavior by **Ris** over **V** is reiterated in the carboxyfluorescein leakage assay, where **Ris** has a greater antagonistic effect than **V** on the pore formation of nisin. Evidently, target recognition is not the sole basis for the higher antimicrobial activity exhibited by **Ris** in the MICs.

Although, the molecules **V** and **Ris** originate from the same class, diverse structural features may contribute to different antibacterial activities. One such structural difference between **Ris**, and **V** lies in the number and size of the carbohydrate moieties linked to the heptapeptide backbone. **Ris** contains six sugars, whereas **V** contains only two. In contrast **Aglu** is stripped of the disaccharide. Given the MS results presented here, **V** has a greater affinity for the bacterial cell-wall target compared to **Ris**. If no carbohydrates are present, as in **Aglu**, a loss of affinity for the target as well as a decrease in activity occurs. In the case of a glycopeptide antibiotic containing several sugars, such as **Ris**, the affinity for the cell wall target decreases while the antibiotic activity remains slightly greater than that of **V**. **Avo**, which contains five sugars, also exhibits a slightly higher efficacy with decreased ligand affinity compared to **V**. The diminished molecular recognition is clearly compensated for by a secondary mechanism. In light of our data, it is likely that the antibiotic efficacy observed for **Ris** and **Avo** may have significant contributions from these surplus carbohydrate moieties, more so than in **V**. It is possible that the excess sugar residues further interfere with the bacterial cell-wall synthesis machinery in the *trans*-glycosylation step, once the glycopeptide antibiotic has docked onto the D-Ala-D-Ala target. Another mechanism that influences efficacy may be that of dimerization. However, as the above-mentioned antibiotics

do not selfassociate easily in solution, we can overrule the possibility of dimer formation.

Although **V** does not selfassociate easily in solution ( $K_{\text{dim}} = 700 \text{ M}^{-1}$ ),<sup>[41]</sup> noncovalent dimerization has been suggested to dramatically increase the effectiveness of some glycopeptides (e.g. eremomycin).<sup>[39]</sup> It has also been demonstrated that cooperativity may induce glycopeptide antibiotics to dimerize upon attaching bacterial cell-wall-mimicking peptides.<sup>[10]</sup> We have included the synthesized head-to-head covalent dimer of vancomycin, **V<sub>D</sub>**, to assess the effect of dimerization on antibiotic activity. In this report, ESI-MS revealed distinct dimerization behavior of **V<sub>D</sub>** in the presence of LII as compared to KAA. At high concentrations of KAA, **V<sub>D</sub>** forms dimers with all four sites occupied with ligand whilst no dimerization could be observed for LII. It is intriguing that, while **V<sub>D</sub>** was already a covalent dimer, the motif of cooperativity and ligand binding manifested itself in the presence of KAA. However, when LII was used as ligand, complex formation with **V<sub>D</sub>** was only extended to the total occupation of the binding sites and does not induce dimerization.

Since LII is structurally closer to the bacterial cell-wall target of glycopeptide antibiotics, it is uncertain whether dimerization actually occurs in vivo. In fact Kim et al.<sup>[42]</sup> have recently demonstrated by rotational-echo double resonance of vancomycin binding sites in *Staphylococcus aureus* that glycopeptide antibiotics might not form dimers in-situ in mature peptidoglycan. Furthermore, they postulate that the sugar interactions with the glycans of the cell wall stabilize the monomeric complex. They stipulate, however, that their conclusion may not necessarily be true for glycopeptide antibiotic binding to immature cell walls and lipid II. In the work presented here, the spontaneous noncovalent dimerization of **V<sub>D</sub>** is specific to KAA and not necessarily correlated to antimicrobial activity. It is likely that antibiotic binding of KAA induces conformational changes in **V<sub>D</sub>** such that it allows dimerization to occur. It is probable then that the drastic inhibition of nisin's activity by **V<sub>D</sub>** is indicative of interference of cell wall growth beyond multiple ligand binding (e.g. steric hindrance).

Obviously, **V<sub>D</sub>** is capable of attaching more ligand than the other glycopeptide monomers, exclusive of the possibility of spontaneous noncovalent dimer formation. Whether both binding sites will be used in vivo for binding to the cell wall is questionable. More work is necessary to truly elucidate whether cooperativity plays a role in vivo, or whether it is induced by a bacterial cell-wall mimic such as KAA.

## Conclusion

We have investigated, for the first time, the noncovalent interactions of a set of glycopeptide antibiotics with a novel water-soluble variant of lipid II (LII), which is a more realistic representation of the target on the bacterial cell wall than the traditionally used *N,N'*-diacetyl-L-lysyl-D-alanyl-D-alanine peptide (KAA). We observed that several antibiotics behave differently towards KAA as compared to LII, both in the magnitude of the interactions and in the effect on dimeriza-

tion. From our data with the more realistic cell-wall-mimicking molecule LII, the mode via which dimerization enhances in-vivo efficacy is questionable. Although our data reveal that dimerization is probably not an important factor in the antibiotic efficacy, they do further emphasize the concept that the sugar moieties attached to some of the antibiotics positively affect the binding to the bacterial cell-wall target and in-vivo efficacy.

## Experimental Section

**Materials:** Vancomycin·HCl, ristocetin A, *N,N'*-diacetyl-L-lysyl-D-alanyl-D-alanine (KAA), and *p*-xylylenediamine were obtained from Sigma-Aldrich. Avoparcin was a gift from M. Siegel at Wyeth Ayerst. (Benzo-triazol-1-yloxy)tris(dimethylamino)phosphonium hexafluorophosphate (BOP) was obtained from A.G. Scientific. Deionized water was used to make up sample solutions and mobile phases for HPLC. All solvents and buffer solutions were HPLC grade. Nisin Z was produced by batch fermentation and purified as previously described.<sup>[43]</sup> Full-length and water-soluble lipid II was prepared by the procedure outlined in the work of Breukink et al.<sup>[28]</sup> Carboxyfluorescein was purchased from Kodak and purified as described.<sup>[44]</sup> Vesicles were prepared as described in literature.<sup>[11]</sup> *Micrococcus flavus* indicator strain DSM 1790 was grown at 30 °C in Mueller–Hinton broth.

**Synthesis of CDP-I from vancomycin:** CDP-I was generated from vancomycin by thermal degradation. Vancomycin·HCl in aqueous solution (1 mg mL<sup>-1</sup>) was heated at 80 °C for 16 h. The sample was purified by semipreparative reversed-phase HPLC (Alltech Adsorbosphere XL C18, 1.0 × 25 cm, 10 μm particles, mobile phase A: 0.1% TFA in H<sub>2</sub>O, mobile phase B: 0.1% TFA in H<sub>2</sub>O/CH<sub>3</sub>CN (5:95) isocratic 20%B, 5 mL min<sup>-1</sup>, UV detection, λ = 280 nm) to afford CDP-I as a white powder.

**Degradation of vancomycin to form aglucovancomycin:** Aglucovancomycin was generated from vancomycin as outlined by Boger et al.<sup>[45]</sup> Vancomycin·HCl (99.55 mg) was treated with trifluoroacetic acid (26 mL) and the resulting solution was stirred (8 h at 50 °C). The mixture was lyophilized and the resulting residue washed with EtOAc/hexane(1:1, 64 mL). The resulting precipitate was collected by filtration. EtOAc (50 mL) was used to wash the filtrate. The filtrate was collected and dried under vacuum. A sample of crude residue was purified by semipreparative reversed-phase HPLC (Alltech Adsorbosphere XL C18, 1.0 × 25 cm, 10 μm particles, mobile phase A: 0.1% TFA in H<sub>2</sub>O, mobile phase B: 0.1% TFA in H<sub>2</sub>O/CH<sub>3</sub>CN (5:95) isocratic 20%B, 5 mL min<sup>-1</sup>, UV detection, λ = 280 nm) to afford pure aglucovancomycin as a white powder.

**Synthesis of ring-closed imidazolidinone derivative of vancomycin (V\*):** Vancomycin·HCl (5.3 mg) was incubated for one week at room temperature in water/methanol (1:1, 5.30 mL) to which formaldehyde solution was added (6 μL, 37% solution stabilized with 15% methanol). The conversion to the ring-closed imidazolidinone derivative of vancomycin was monitored by mass spectrometry.<sup>[25]</sup> The sample was purified by semipreparative reversed-phase HPLC (Alltech Adsorbosphere XL C18, 1.0 × 25 cm, 10 μm particles, mobile phase A: 0.1% TFA in H<sub>2</sub>O, mobile phase B: 0.1% TFA in H<sub>2</sub>O/CH<sub>3</sub>CN (5:95) isocratic 20%B, 5 mL min<sup>-1</sup>, UV detection, λ = 280 nm).

**Synthesis of covalently linked vancomycin dimer (V<sub>D</sub>):** A dimer of vancomycin was synthesized following a procedure described in the literature<sup>[46]</sup> with some modification. In our procedure, BOP was used to catalyze the reaction, resulting in two products only—the desired covalent dimer and the linker-attached monomer. *p*-Xylylenediamine was chosen as the linker in the dimeric derivative because it is structurally rigid and easily modified synthetically. To a solution of vancomycin hydrochloride (100 mg) in DMF/DMSO (1:1, 1 mL) was added a solution of *p*-xylylenediamine (4.5 mg, 0.5 equiv) in DMSO (0.5 mL). The mixture was shaken until it had completely dissolved. BOP (30 mg, 1 equiv) was dissolved in DMF (0.5 mL). Both mixtures were cooled to ≈0 °C then combined. DIPEA (12 μL, 1 equiv) was added. The solution was stirred overnight at room temperature.

A sample of crude residue was purified by semipreparative reversed-phase HPLC (Alltech Adsorbosphere XL C18, 1.0 × 25 cm, 10 μm particles, mobile phase A: 0.1% TFA in H<sub>2</sub>O, mobile phase B: 0.1% TFA in H<sub>2</sub>O/CH<sub>3</sub>CN (5:95) 5 mL min<sup>-1</sup>, UV detection, λ = 280 nm) to afford pure covalently linked vancomycin dimer as a white powder. Separations were accomplished using the following gradient conditions: 2% B for 3 min to 50% B in 30 min, hold for 2 min, then to 90% B in 5 min, hold for 2 min, and return to 2% B in 2 min.

**Synthesis and purification of water-soluble lipid II (LII) containing a polyprenyl chain of 3 isoprene units:** Water-soluble lipid II was created according to a procedure based on the addition of farnesyl phosphate to a membrane preparation of *Micrococcus flavus* in the presence of suitable amounts of substrates and will be described in detail elsewhere.<sup>[28]</sup> Farnesyl-lipid II, water-soluble lipid II containing 3 isoprene units, was stored in methanol at -20 °C at a concentration of 0.35 mM.

**Mass spectrometry:** Electrospray mass spectra were recorded with a time-of-flight (LCT) mass spectrometer fitted with a Z-spray nanoflow ion source (Micromass Ltd., Manchester, UK). Each of the glycopeptide antibiotics, KAA and LII were dissolved in 25 mM ammonium acetate (acidified with acetic acid to pH 5.2). In an initial screening process to determine whether the noncovalent complexes of the glycopeptide antibiotics with KAA or LII could be observed by mass spectrometry, 100 picomoles of each antibiotic was combined with an equivalent amount of ligand (concentration ranges between 10 and 20 μM, depending on the molecular mass of the receptor). For further titration experiments, a 10 μM amount of antibiotic was added to a range of KAA and LII concentrations (1, 2, 4, 8, 16, 32 μM). The capillary voltage was typically 1200 V and the cone voltage was between 10 and 15 V. The source block temperature was maintained at 75 °C. Spectra were acquired and processed with Micromass MassLynx version 3.4 software. In order to obtain the peak areas required to calculate relative binding constants by mass spectrometry, spectra were combined and the background was subtracted. Subsequently, the data was smoothed and centred. All data was handled in a similar manner, unless otherwise stated. Solution-phase association constants for glycopeptide antibiotics were determined by mass spectrometry by means of procedures described previously.<sup>[13, 14, 29, 35, 47]</sup> Binding constants were derived from single spectra<sup>[29]</sup> or from titration experiments.

**Carboxyfluorescein leakage (CF) experiments:** CF-loaded vesicles containing 0.1% LII were prepared as described.<sup>[48]</sup> The inhibitive effect of the glycopeptide antibiotics on the pore formation by nisin was measured by monitoring the nisin-induced leakage of carboxyfluorescein from model membrane vesicles in the presence of increasing glycopeptide antibiotic concentrations. Initially, the glycopeptide antibiotic (0–50 μM) was preincubated (3 min) with CF-loaded vesicles (5 μM based on lipid-P<sub>i</sub> content). Then nisin (5 nM) was added. The nisin-induced leakage of carboxyfluorescein from the vesicles was monitored by measuring the increase in fluorescence intensity at λ = 515 nm (excitation at 492 nm) with a SPF500 C spectrophotometer (SLM instruments Inc., USA) at 20 °C.

**Minimum inhibitory concentration (MIC) determination:** The minimum inhibitory concentration was determined by measuring the inhibition of growth of the indicator strain *Micrococcus flavus* DSM 1790 by serial dilution in a Mueller–Hinton broth. In microtiter plates, 1:1 dilution series of the appropriate antibiotic were made and each well was inoculated with a fresh culture of bacteria. The total volume per well was 200 μL. The plates were incubated overnight at 30 °C prior to recording the MICs.

## Acknowledgement

The authors would like to thank Kees Versluis and Dirk Rijkers for their helpful discussions and suggestions regarding the synthesis of the dimer.

- [1] K. C. Nicolaou, C. N. C. Boddy, S. Bräse, N. Winssinger, *Angew. Chem.* **1999**, *111*, 2230–2287; *Angew. Chem. Int. Ed.* **1999**, *38*, 2096–2152.
- [2] G. Zubay in *Biochemistry* (Ed.: K. Kane), W. C. Brown Publishers, Indiana, **1993**, pp. 605–611.
- [3] A. N. Chatterjee, H. R. Perkins, *Biochem. Biophys. Res. Commun.* **1966**, *24*, 489–494.

- [4] C. T. Walsh, *Science* **1993**, *261*, 308–309.
- [5] J. P. Mackay, U. Gerhard, D. A. Beauregard, R. A. Maplestone, D. H. Williams, *J. Am. Chem. Soc.* **1994**, *116*, 4573–4580.
- [6] U. Gerhard, J. P. Mackay, R. A. Maplestone, D. H. Williams, *J. Am. Chem. Soc.* **1993**, *115*, 232–237.
- [7] J. P. Mackay, U. Gerhard, D. A. Beauregard, M. S. Westwell, M. S. Searle, D. H. Williams, *J. Am. Chem. Soc.* **1994**, *116*, 4581–4590.
- [8] K. C. Nicolaou, R. Hughes, S. Y. Cho, N. Winssinger, H. Labischinski, R. Endermann, *Chem. Eur. J.* **2001**, *7*, 3824–3843.
- [9] M. A. Cooper, D. H. Williams, *Chem. Biol.* **1999**, *6*, 891–899.
- [10] D. H. Williams, A. J. Maguire, W. Tszuki, M. S. Westwell, *Science* **1998**, *280*, 711–714.
- [11] E. Breukink, I. Wiedemann, C. van Kraaij, O. P. Kuipers, H.-G. Sahl, B. de Kruijff, *Science* **1999**, *286*, 2361–2364.
- [12] H. Brötz, M. Josten, I. Wiedemann, U. Schneider, F. Götz, G. Bierbaum, H.-G. Sahl, *Mol. Microbiol.* **1998**, *30*, 317–329.
- [13] A. van der Kerk-van Hoof, A. J. R. Heck, *J. Antimicrob. Chemother.* **1999**, *44*, 593–599.
- [14] T. Staroske, D. P. O'Brien, T. J. D. Jørgensen, P. Roepstorff, D. H. Williams, A. J. R. Heck, *Chem. Eur. J.* **2000**, *6*, 504–509.
- [15] T. J. D. Jørgensen, T. Staroske, P. Roepstorff, D. H. Williams, A. J. R. Heck, *J. Chem. Soc. Perkin Trans. 2* **1999**, 1859–1863.
- [16] A. van der Kerk-van Hoof, A. J. R. Heck, *J. Mass Spectrom.* **1999**, *34*, 813–819.
- [17] C. M. Pearce, U. Gerhard, D. H. Williams, *J. Chem. Soc. Perkin Trans. 2* **1995**, 159–162.
- [18] M. P. Williamson, D. H. Williams, S. J. Hammond, *Tetrahedron* **1984**, *40*, 569–577.
- [19] D. H. Williams, D. W. Butcher, *J. Am. Chem. Soc.* **1981**, *103*, 5697–5700.
- [20] A. M. A. van Wageningen, T. Staroske, D. H. Williams, *Chem. Commun.* **1998**, 1171–1172.
- [21] M. A. Cooper, M. T. Fiorini, C. Abell, D. H. Williams, *Bioorg. Med. Chem.* **2000**, *8*, 2609–2616.
- [22] F. Bager, M. Madsen, J. Christensen, F. M. Aarestrup, *Prev. Vet. Med.* **1997**, *31*, 95–112.
- [23] B. E. Murray, *Emerg. Infect. Dis.* **1998**, *4*, 37.
- [24] R. Nagarajan, *Glycopeptide Antibiotics*, Marcel Dekker, New York, **1994**.
- [25] A. J. R. Heck, P. J. Bonnici, E. Breukink, D. Morris, M. Wills, *Chem. Eur. J.* **2001**, *7*, 910–916.
- [26] C. M. Harris, H. Kopecka, T. M. Harris, *J. Am. Chem. Soc.* **1983**, *105*, 6915–6922.
- [27] P. J. Bonnici, M. Damen, J. C. M. Waterval, A. J. R. Heck, *Anal. Biochem.* **2001**, *290*, 292–301.
- [28] E. Breukink, H. E. van Heusden, P. J. Vollmerhaus, E. Swieczewska, L. Brunner, S. Walker, A. J. R. Heck, B. de Kruijff, unpublished results, **2002**.
- [29] T. J. D. Jørgensen, P. Roepstorff, A. J. R. Heck, *Anal. Chem.* **1998**, *70*, 4427–4432.
- [30] E. Leize, A. Jaffrezic, A. van Dorsselaer, *J. Mass Spectrom.* **1996**, *31*, 537–544.
- [31] J. A. Loo, *Int. J. Mass Spectrom.* **2000**, *200*, 175–186.
- [32] P. Groves, M. S. Searle, J. P. Waltho, D. H. Williams, *J. Am. Chem. Soc.* **1995**, *117*, 7958–7964.
- [33] D. H. Williams, M. P. Williamson, D. W. Butcher, S. J. Hammond, *J. Am. Chem. Soc.* **1983**, *105*, 1332–1339.
- [34] H. R. Perkins, *Biochem. J.* **1969**, *111*, 195–205.
- [35] H.-K. Lim, Y. L. Hsieh, B. Ganem, J. Henion, *J. Mass Spectrom.* **1995**, *30*, 708–714.
- [36] A. Rodríguez-Tebar, D. Vázquez, J. L. P. Velázquez, J. Laynez, I. Wadsö, *J. Antibiot.* **1986**, *39*, 1578–1583.
- [37] R. Kannan, C. M. Harris, T. M. Harris, J. P. Waltho, N. J. Skelton, D. H. Williams, *J. Am. Chem. Soc.* **1988**, *110*, 2946–2953.
- [38] J. Kaplan, B. D. Korty, P. H. Axelsen, P. J. Loll, *J. Med. Chem.* **2001**, *44*, 1837–1840.
- [39] P. Groves, M. S. Searle, J. P. Mackay, D. H. Williams, *Structure* **1994**, *2*, 747–754.
- [40] H. Shiozawa, B. C. S. Chia, N. L. Davies, R. Zerella, D. H. Williams, *J. Am. Chem. Soc.* **2002**, *124*, 3914–3919.
- [41] U. N. Sundram, J. H. Griffin, *J. Am. Chem. Soc.* **1996**, *118*, 13107–13108.

- [42] S. J. Kim, L. Cegelski, D. R. Studelska, R. D. O'Connor, A. K. Mehta, J. Schaefer, *Biochemistry* **2002**, *41*, 6967–6977.
- [43] O. P. Kuipers, H. S. Rollema, W. M. G. J. Yap, H. J. Boot, R. J. Siezen, W. M. de Vos, *J. Biol. Chem.* **1992**, *267*, 24340–24346.
- [44] E. Ralston, L. M. Hjelmeland, R. D. Klausner, J. N. Weinstein, R. Blumenthal, *Biochim. Biophys. Acta* **1981**, *649*, 133–137.
- [45] D. L. Boger, S. Miyazaki, O. Loiseleur, R. T. Beresis, S. L. Castle, J. H. Wu, Q. Jin, *J. Am. Chem. Soc.* **1998**, *120*, 8920–8926.
- [46] J. Rao, G. M. Whitesides, *J. Am. Chem. Soc.* **1997**, *119*, 10286–10290.
- [47] K. A. Sannes-Lowery, R. H. Griffey, S. A. Hofstadler, *Anal. Biochem.* **2000**, *280*, 264–271.
- [48] I. Wiedemann, E. Breukink, C. van Kraaij, O. P. Kuipers, G. Bierbaum, B. de Kruijff, H.-G. Sahl, *J. Biol. Chem.* **2001**, *276*, 1772–1779.

Received: September 25, 2002 [F4454]